Applied Surface Science 255 (2009) 8483–8487

Contents lists available at ScienceDirect

Applied Surface Science

journal homepage: www.elsevier.com/locate/apsusc

Fabrication of micro-gratings on Au–Cr thin film by femtosecond laser interference with different pulse durations

Xianhua Wang, Feng Chen *, Hewei Liu, Weiwei Liang, Qing Yang, Jinhai Si, Xun Hou

Key Laboratory for Physical Electronics and Devices of the Ministry of Education & Key Laboratory of Photonics Technology for Information, Shaanxi Province, School of Electronics and Information Engineering, Xi'an Jiaotong University, No. 28, Xianning West Road, Xi'an 710049, P.R. China

ARTICLE INFO

Article history:
Received 22 February 2009
Received in revised form 28 April 2009
Accepted 2 June 2009
Available online 21 June 2009

Keywords:
Femtosecond laser pulse
Interference
Periodic microstructures
Surface relief micro-grating
Metal thin film

ABSTRACT

We encoded surface relief micro-gratings on Au–Cr thin films using two-beam interference of femtosecond laser pulses with the durations from 25 fs to 70 fs. The dependence of the fabrication quality on the pulse duration has been investigated both numerically and experimentally. The results revealed that the shorter pulses were preferable to prepare periodical microstructures with minimal ablation fringe width and satisfied fabrication quality. This work has potential applications on periodic functional microstructures fabrication for ultra-fine processing and modification on various materials, especially for intractable materials.

1. Introduction

Artificial periodic microstructures have been attracted great interest due to their promising applications in communication, sensing, conduction, filtering and resonance [1–5]. A variety of technologies were used to fabricate these microstructures, such as self-assembling [6], direct laser writing [7], microcontact printing [8], phase mask [9], and laser interference [10–12]. Among them, laser interference is a highly efficient method for fabricating periodic microstructures because it can be controlled easily by changing the number and arrangement of the coherent laser beams to fabricate diverse two- and three-dimensional periodic microstructures on various materials.

Femtosecond laser pulse, with its rapid developments over past decades, becomes a powerful tool for micro-fabrication and micromachining of many multi-functional structures on the surface of samples or inside transparent materials [13–15]. It is extremely short in time domain, leading to very high peak power and very intense non-linear effects. Many groups have reported the successful fabrication of periodical structures in various materials by coherent multiple femtosecond laser pulses. Furthermore, the peak power and non-linear effects will be the intensified when the pulse duration becomes shorter, which is preferable to fabricate superfine microstructures on intractable materials, such as glasses, quartz, metals and ceramics. However, most of the pulse durations applied to the laser interference fabrications employed in previous works, as we know, were longer than 120 fs [10–12,16–17]. The processing characteristics and fabrication properties of using sub-100 fs pulses have been seldom reported. Investigating the relationship between pulse duration and its fabrication quality in sub-100 fs time domain is very helpful to optimize parameters in practical possessing based on material features and technical specifications in the relative higher peak power range.

In this letter, we report the fabrication of surface relief micro-gratings on Au–Cr thin films using two-beam interference of femtosecond laser pulses with the durations from 25 fs to 70 fs. The micro-morphologies and diffractive performances of encoded micro-gratings have been characterized. The dependence of fabrication properties on pulse duration was studied in detail both numerically and experimentally.

2. Experimental setup

Fig. 1 shows our experimental setup. Near infrared light pulses generated from a model-locked Ti: sapphire multi-pass amplifying system (central wavelength: 800 nm, pulse duration: 25–200 fs, repetition rate: 1 kHz; FEMTOPOWER compact Pro, FEMTOLASERS) were split into two beams by a beam splitter (BS), and then crossed on the surface of sample to give a spot size of ~150 μm in diameter. We employ dedicated adjustable delay line and the sum-frequency generation method using non-linear optical crystals such as β-barium borate (BBO) to adjust and achieve the

* Corresponding author. Tel.: +86 029 82665105; fax: +86 029 82665105.
E-mail address: chenfeng@mail.xjtu.edu.cn (F. Chen).

0169-4332/$ – see front matter © 2009 Elsevier B.V. All rights reserved.
doi:10.1016/j.apsusc.2009.06.057

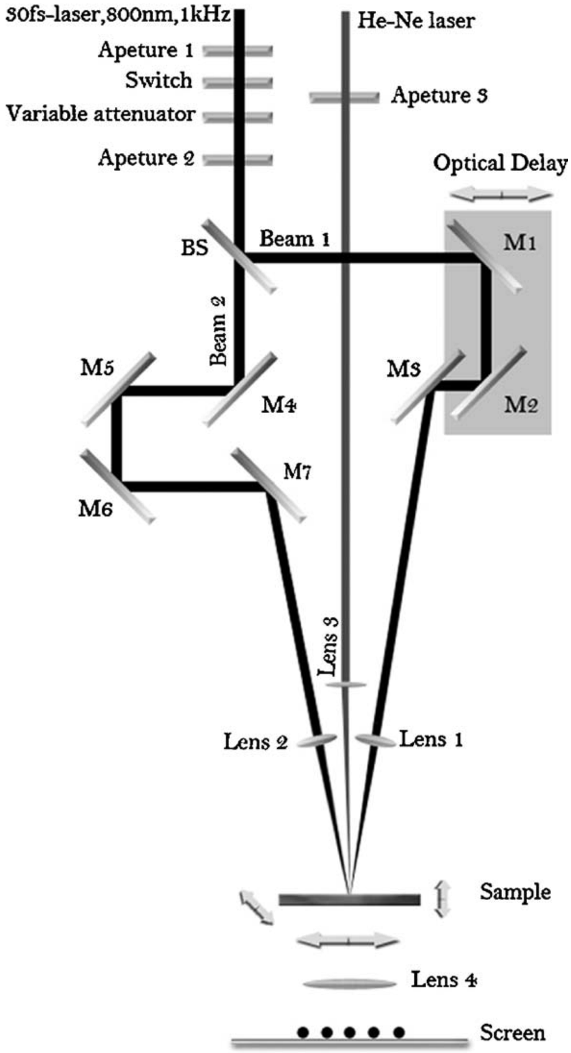

Fig. 1. Experimental setup. It consists of a femtosecond laser resource, a variable attenuator, a mechanical shutter, a beam splitter (BS, $R = 0.5$), and an optical delay. The sample was positioned on a mechanical 3D stage.

interference of femtosecond laser pulses. The mechanical shutter is employed to control the irradiating time, the incident laser power can be varied by rotating the variable attenuator and adding/removing attenuation slices. In our experiments, the colliding angle between the two beams, θ, was fixed about 21.3°.

For the sample, Au–Cr thin film, Au layers with thickness of about 100 nm were sputter-deposited on glass substrates coated with a Cr layer about 50 nm thick. Cr layer was formed between the Au film and the glass, which is in order to enhance the adhesion of Au film to glass substrate due to the adhesive force of Au film to the substrate such as glass is very weak.

3. Results and discussion

The femtosecond laser pulses employed in our experiments have much wider spectrum widths, usually more than 50 nm (FWHM), comparing to less than 20 nm for 150 fs pulses. Moreover, for CPA (chirped-pulse amplification) systems, adjusting the compressor to change pulse duration has little effect on its spectrum [18,19]. It is reasonable to use a static spectrum distribution for numeral simulations. For a pulse with spectrum distribution function $F(\nu)$ split into two pulses by a beam splitter ($\nu = c/\lambda$, where ν is the light frequency, c is the speed of light in the medium and λ is the wavelength), their complex electric field intensities, υ_1 and υ_2, can be expressed spatially by the sum of each spectrum component:

$$\upsilon_1(x,y) = \sum_{\nu} A_1 F(\nu) \exp\left[-\frac{x^2+y^2}{\omega_0^2}\right], \tag{1}$$

$$\upsilon_2(x,y) = \sum_{\nu} A_2 F(\nu) \exp\left[-\frac{x^2+y^2}{\omega_0^2}\right], \tag{2}$$

where x and y are the spatial coordinates, A_1 and A_2 are the light amplitudes of the two pulses respectively, and ω_0 is the diameter of the focal spot. In the case of the beam splitter's reflectivity is 0.5, $A_1 = A_2 = A$. The spectrum distribution function $F(\nu)$ can be expressed as

$$F(\nu) = \frac{f(\nu)}{\sqrt{2(\alpha+i\beta)}} \exp\left[-\frac{(\nu-\nu_0)^2}{4(\alpha+i\beta)}\right], \tag{3}$$

for $f(\nu)$ is the actual spectrum intensity distribution which can be measured by a spectrometer, $\alpha = 2\ln 2/\tau^2$ is pulse duration parameter determined by the pulse duration τ, and β is chirp parameter determined by individual CPA system. When the two pulses collided temporally and spatially, the intensity distribution of interferen ce pattern is given by

$$I = \sum_{\nu}\left[|\upsilon_1|^2 + |\upsilon_2|^2 + (\upsilon_1^*\upsilon_2 + \upsilon_2^*\upsilon_1)\cos\delta\right], \tag{4}$$

as $\delta = (2\pi/\lambda)x\sin\frac{\theta}{2}$ is the optic path difference determined by the spatial location x. The calculated results were shown in Fig. 2a, d, g and j. The central point of the interference pattern was set as origin (0, 0), and the side length of simulation range was 120 μm (from −60 μm to 60 μm). The relative intensity distribution curve at $y = 0$ has also been plotted, as shown in Fig. 2b, e, h and k.

For two laser pluses crossed at angle θ, the size of the overlap area is given by $c\tau\,(\mathrm{Sin}\,\theta/2)^{-1}$; the number of interference fringes produced by two pluses is independent of the angle and, for transform-limited pulses, is roughly $2c\tau/\lambda$ [20,21]. We varied the durations of laser pulses by adjusting the prism compressor, and measured the pulses durations by an autocorrelator (Femtometer, FEMTOLASERS). In our experiments, the selected pulse durations and the corresponding incident laser energies were: 0.4 J/cm^2 for 25 fs, 0.45 J/cm^2 for 35 fs, 0.9 J/cm^2 for 60 fs and 1.6 J/cm^2 for 70 fs. Respectively, there were 18, 26, 45 and 52 fringes produced theoretically; 14, 20, 40 and 48 fringes produced in experiments, as shown in Fig. 2c, f, i and l. This difference mainly stemmed from the ablation threshold effect and Gaussian distribution of laser beams' intensities. For a Gaussian laser beam, the energy density of central region is much higher than the edge. When the central energy density exceeded the ablation threshold of material, the energy density toward edge may still remains below the threshold. And this ablation threshold will not be considered in the above formula.

The period of encoded micro-grating is about 2.2 μm, which agreed well with the calculated result by $\lambda\,(2\mathrm{Sin}\,\theta/2)^{-1} \approx 2.16$ μm with $\lambda = 800$ nm and $\theta = 21.3^\circ$. Fig. 3 shows the micro-morphology of the micro-grating encoded on Au–Cr thin film imaged by a color 3D laser scanning microscope (VK9710, Keyence). The pulse duration and laser energy were 40 fs and 0.5 J/cm^2, respectively. Compared to the fringes toward the edge, the fringes near the center of the grating were wider and deeper. This phenomenon probably can be attributed to the following two reasons. First, the energy density distribution difference of Gaussian laser beam induced asymmetry is dominant reason. Second, the interfered fringes produced by different components in spectrum of the laser pulses will separated from each other expect in the location of central bright fringe, so the energies of bright interfered fringes dispersed to a relative wider range, and which will be intensified

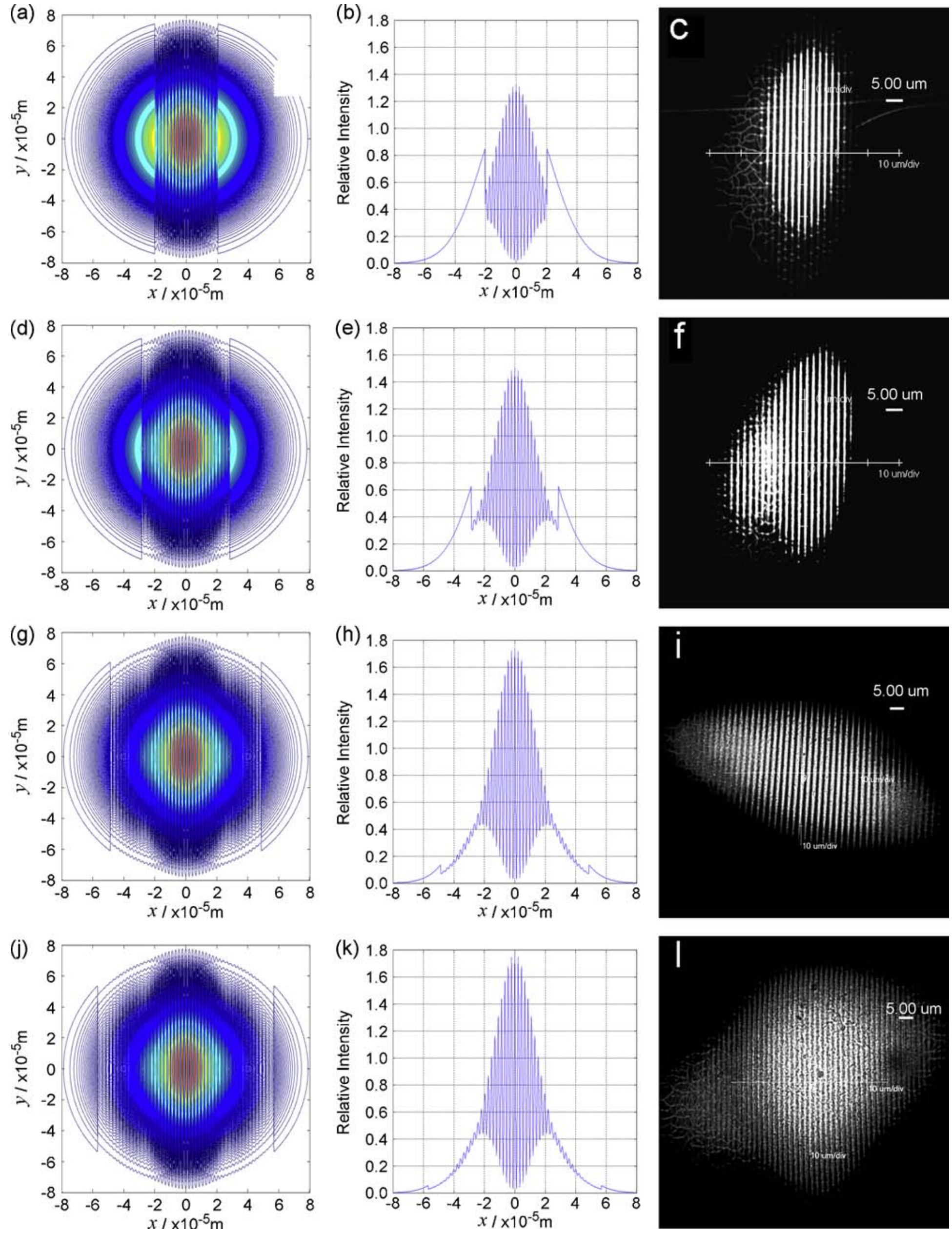

Fig. 2. The dependence of interference patterns on pulse durations (a∼c) 25 fs; (d∼f) 35 fs; (g∼i) 60 fs; (j∼l) 70 fs. (a), (d), (g) and (j) are the energy distribution contour plans; (b), (e), (h) and (k) are the relative intensity distribution curves at $y = 0$; (c), (f), (i) and (l) are the optical microscope images of experimental results (tungsten light source, through illumination, same light intensity). The calculated numbers of interference fringes, experimental results and incident laser energies for corresponding pulse durations were as follows: 18, 14, 0.4 J/cm^2 for 25 fs; 26, 20, 0.45 J/cm^2 for 35 fs; 45, 40, 0.9 J/cm^2 for 60 fs; 52, 48, 1.6 J/cm^2 for 70 fs.

toward the edge. This energy dispersion induced the decrease of energy density will influence the width and depth of ablation.

Fig. 4 shows the diffractive pattern of 48 fringes micro-gratings encoded by interfered two 70 fs pulses (as shown in Fig. 2l) for He–Ne laser (λ = 632.8 nm). The calculated light intensity distribution of diffractive pattern was shown in Fig. 4a, the zero order diffractive light intensity was about 2.5 times versus the first order; the actual diffractive pattern was shown in Fig. 4b, and the zero order diffractive light intensity (75 nW) was about three times to the first order (25 nW).

From the calculated and experimental results illustrated above, we can observe that the shorter pulses (such as 25 fs and 35 fs) were preferable to prepare periodical microstructures compared to longer pulses (such as 60 fs and 70 fs). For shorter pulse durations, the interference of two laser pulses takes place in a limited region, which is always smaller than the focal spot, as shown in Fig. 2a and d. And there are very small differences between the maximal intensity of bright interfered fringes and the maximum intensity out of interfered area, as shown in Fig. 2 and e. When incident energy is well above the ablation threshold influence of materials, it may lead to unexpected damages out of the interfered area. Consequently, we should precisely optimize pulse energy and irradiation time to avoid redundant ablation. In this case, the laser influence is slightly exceeded the ablation threshold, which is very helpful to prepare microstructures with minimal ablation fringe width, as shown in Fig. 2c and f. Compared to the shorter-pulse-duration process, the interfered area of two laser beams with longer pulse durations is enlarged, as shown in Fig. 2g and j. The laser energy is concentrated in the interfered area, and the peak intensities of bright interfered fringes in the enlarged area are very

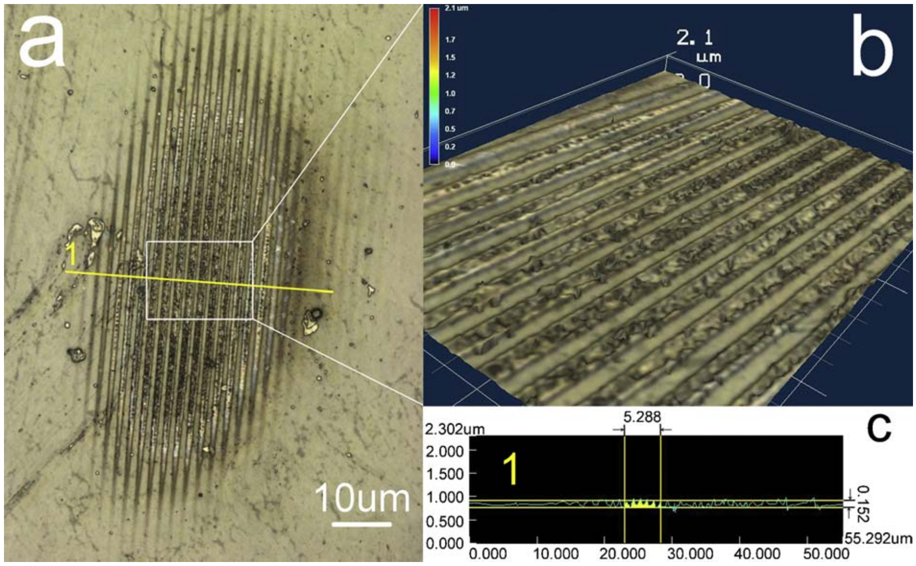

Fig. 3. The micro-morphology of the micro-grating encoded on Au–Cr thin film. The pulse duration and laser energy were 40 fs and 0.5 J/cm^2 respectively. (a) The laser microscope image of micro-grating, which period was about 2.2 μm; (b) the color 3D morphology image of local part (the denoted rectangle area in (a)); (c) the cross section profile of micro-grating in the direction of line 1 shown in (a).

low, as shown in Fig. 2h and k. To obtain higher processing efficiency, more laser energy should be injected into the sample to ensure all the intensities of bright interfered fringes are well above the ablation threshold, which is indicated that the ablation widths induced by bright interfered fringes will be expanded in the *x*-axis direction, as shown in Fig. 2i and l. On the other hand, however, the intensities of dark interfered fringes are increased synchronously, which may lead undesirable ablation on glass substrate in the central location of focal spot, especially as shown in Fig. 2l. As a result, suitable pulse durations shall be selected to obtain fine spatial resolution with highly processing efficiency in practice.

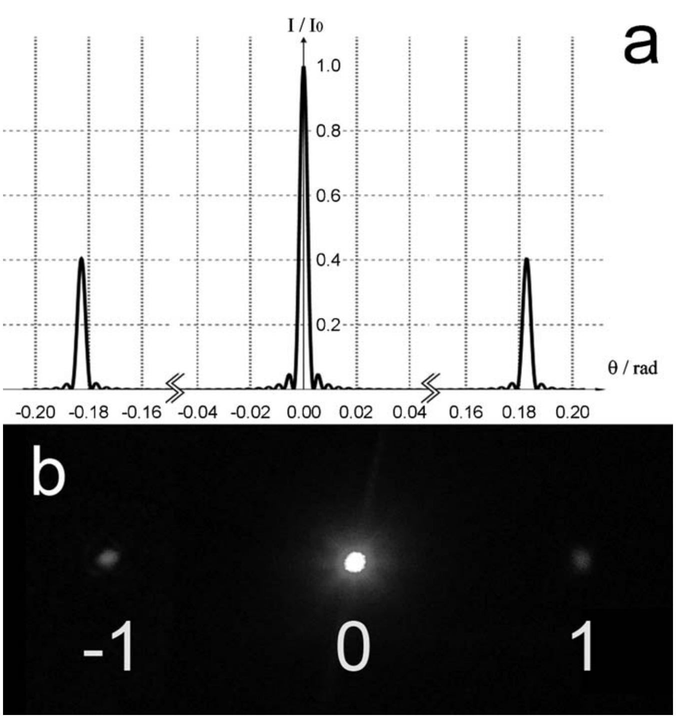

Fig. 4. The diffractive pattern of 48 fringes micro-gratings encoded by interfered 70 fs pulses (as shown in Fig. 2l) for He–Ne laser (λ = 632.8 nm). (a) The calculated intensity of diffractive pattern; (b) the actual diffractive pattern.

4. Conclusions

We have performed a detailed study on the micro-gratings encoded on the surface of Au–Cr thin film using two-beam interference of femtosecond pulses with the durations from 25 fs to 70 fs both theoretically and experimentally. The experimental results and numeral analysis indicated that the durations of laser pulses in this time domain will influence the qualities of encoded gratings significantly. For shorter pulse durations, process was implemented under the condition that the laser influence was slightly exceeded the ablation threshold, which was helpful to produce microstructures with fine resolution. Furthermore, using shorter laser pulses is easy to achieve higher peak power and less thermal effects, and the non-linear effects such as threshold effects will be intensified, which is favorable to implement fine surface processing and modification on various materials, especially for intractable materials. In contrast, for longer pulse durations, the enlargement of interfered areas can improve the processing efficiency, which is convenient to fabricating large-area periodical microstructures with high efficiency. But the fabrication quality will be reduced due to the expanded ablation fringes width and the redundant ablation in the locations of dark interfered fringes. These disadvantages will restrict their applications on some intractable materials. Practically, it is efficient and economical to fabricate or modify samples by selecting adaptive pulse durations.

In addition, the periodicities of interference patterns produced by two coherent beams can be easily changed by varying the cross angle, and large-area periodical microstructures can be prepared by employing a precise 3D moving stage. This is very useful for preparing large-area and periodicity-controllable periodical microstructures.

Acknowledgments

The authors gratefully acknowledge the financial support for this work provided by the National Science Foundation of China under the Grant Nos. 60678011 and 10674107.

References

[1] F. Brechet, P. Roy, J. Marcou, D. Paguoux, Singlemode propagation into depressed-core-index photonic-bandgap fiber designed for zero-dispersion propagation at short wavelengths, Electronics Letters 36 (2000) 514–515.
[2] P. Friebele, E. Joseph, Fiber Bragg grating strain sensors: present and future applications in smart structures, Optics & Photonics News 9 (1998) 33–37.
[3] Guochang Gu, Shiyao Zhu, Xiang Wu, Hong Chen, An active optical multi-channel switch, Chinses Physics Letters 16 (1999) 734–736.
[4] Suxia Yang, J.H. Page, Zhengyou Liu, M.L. Cowan, C.T. Chan, Ping Sheng, Ultrasound tunneling through 3D phononic crystals, Physical Review Letters 88 (2002) 104301.
[5] G.Q. Liang, W.D. Mao, Y.Y. Pu, H. Zou, H.Z. Wang, Fabrication of two-dimensional coupled photonic crystal resonator arrays by holographic lithography, Applied Physics Letters 89 (2006) 041902–041904.
[6] K. Fukuda, H.-B. Sun, S. Matsuo, H. Misawa, Self-organizing three-dimensional colloidal photonic crystal structure with augmented dielectric contrast, Japanese Journal of Applied Physics 37 (1998) L508–L511.
[7] B.H. Cumpston, S.P. Ananthavel, Stephen Barlow, D.L. Dyer, J.E. Ehrlich, L.L. Erskine, A.A. Heikal, S.M. Kuebler, I.-Y.S. Lee, D. McCord-Maughon, Jinqui Qin, Harald Röckel, Mariacristina Rumi, Xiangli Wu, S.R. Marder, J.W. Perry, Two-photon polymerization initiators for three-dimensional optical data storage and microfabrication, Nature 398 (1999) 51–54.
[8] Toby Cornish, D.W. Branch, B.C. Wheeler, J.T. Campanelli, Microcontact printing: a versatile technique for the study of synaptogenic molecules, Molecular and Cellular Neuroscience 20 (2002) 140–153.
[9] P.E. Dyer, R.J. Farley, R. Giedl, Analysis of grating formation with excimer laser irradiated phased masks, Optics Communications 115 (1995) 327–334.
[10] T. Kondo, S. Juodkazis, V. Mizeikis, H. Misawa, S. Matsuo, Holographic lithography of periodic twoand three-dimensional microstructures in photoresist SU-8, Optics Express 14 (2006) 7943–7953.
[11] Masahiro Hirano, Ken-ichi Kawamura, Hideo Hosono, "Encoding of holographic grating and periodic nano-structure by femtosecond laser pulse, Applied Surface Science 197–198 (2002) 688–698.
[12] Tianqing Jia, Motoyoshi Baba, Masayuki Suzuki, R.A. Ganeev, Hiroto Kuroda, Jianrong Qiu, Xinshun Wang, Ruxin Li, Zhizhan Xu, Fabrication of two-dimensional periodic nanostructures by two-beam interference of femtosecond pulses, Optics Express 16 (2008) 1874–1878.
[13] Satoshi Kawata, Hongbo Sun, Tomokazu Tanaka, Kenji Takada, Finer features for functional microdevices: Micromachines can be created with higher resolution using two-photon absorption, Nature 412 (2001) 697–698.
[14] B.N. Chichkov, C. Momma, S. Noltevon, F. Alvensleben, A. Tünnermann, Femtosecond, picosecond and nanosecond laser ablation of solids, Applied Physics A: Material Science & Processing 63 (1996) 109–115.
[15] J. Ihlemann, B. Wolff, R. Simon, Nanosecond and femtosecond excimer laser ablation of fused silica, Applied Physics A 54 (1992) 363–368.
[16] K.H. Baek, J.H. Park, J.H. Kim, C.K. Kim, C.S. Yoon, G.J. Lee, Y.P. Lee, Formation of periodic magnetic structure by localized amorphization of crystalline Co_2MnSi using femtosecond laser, Journal of Applied Physics 103 (2008), 07E701.
[17] J. Bekesi, J. Meinertz, J. Ihlemann, P. Simon, Fabrication of large-area grating structures through laser ablation, Applied Physics A: Materials Science & Processing 93 (2008) 27–31.
[18] V.J. Pino-Robledo, T.A. Hall, Chronocyclic description of laser pulse compression, Optics Commmunication 125 (1996) 338–348.
[19] S. Kane, J. Squier, Prism-pair stretcher-compressor system for simultaneous second-and-third-order dispersion compensation in chirped-pulse amplification, Journal of the Optical Society of America B 14 (1997) 661–665.
[20] A.A. Maznev, T.F. Crimmins, K.A. Nelson, How to make femtosecond pulses overlap, Optics Letters 23 (1998) 1378–1380.
[21] Ken-ichi Kawamura, Naoko Ito, Nobuhiko Sarukura, Masahiro Hirano, Hideo Hosono, New adjustment technique for time coincidence of femtosecond laser pulses using third harmonic generation in air and its application to holograph encoding system, Review of Scientific Instruments 73 (2002) 1711–1714.